https://ntrs.nasa.gov/search.jsp?R=19700015726 2020-03-12T02:38:16+00:00Z

General Disclaimer

One or more of the Following Statements may affect this Document

- This document has been reproduced from the best copy furnished by the organizational source. It is being released in the interest of making available as much information as possible.

- This document may contain data, which exceeds the sheet parameters. It was furnished in this condition by the organizational source and is the best copy available.

- This document may contain tone-on-tone or color graphs, charts and/or pictures, which have been reproduced in black and white.

- This document is paginated as submitted by the original source.

- Portions of this document are not fully legible due to the historical nature of some of the material. However, it is the best reproduction available from the original submission.

Produced by the NASA Center for Aerospace Information (CASI)

CR 73436
AVAILABLE TO THE PUBLIC

SPACE SCIENCES LABORATORY

THEORETICAL CALCULATION OF THE ELECTROMAGNETIC RESPONSE OF A RADIALLY LAYERED MODEL MOON

B. D. Fuller and S. H. Ward

Technical Report on

NASA Contract
NAS 2-4996 ITEM 788

Space Sciences Laboratory Series 10, Issue 24

UNIVERSITY OF CALIFORNIA, BERKELEY

N70-25031
(ACCESSION NUMBER)
30
(PAGES)
(NASA CR OR TMX OR AD NUMBER)
1
(THRU)
1
(CODE)
30
(CATEGORY)
FACILITY FORM 602

Space Sciences Laboratory
University of California
Berkeley, California 94720

THEORETICAL CALCULATIONS OF THE ELECTROMAGNETIC RESPONSE OF A RADIALLY LAYERED MODEL MOON

By

B. D. Fuller and S. H. Ward

Technical Report on

NASA Contract
NAS 2-4996

Space Sciences Laboratory Series 10, Issue 24

THEORETICAL CALCULATIONS OF THE ELECTROMAGNETIC RESPONSE OF A RADIALLY LAYERED MODEL MOON

B. D. Fuller and S. H. Ward

Introduction

The interaction of the moon with an electromagnetic field is important to passive lunar magnetometer experiments which utilize the natural time-varying interplanetary magnetic field and to lunar experiments utilizing a known electromagnetic source. Electromagnetically, the lunar situation is extremely complex; the lunar sphere, thought to be conductive, is immersed in a conducting plasma permeated by a magnetic field (Schwartz, 1967) and, in all probability, both the lunar body and the surrounding medium are anisotropic and inhomogeneous. The exact problem is quite intractable and more simplified models are necessary in order to interpret data collected in magnetic and electromagnetic experiments. Such models have included a plane wave-plane layered half space model (Ward, Jiracek and Linlor, 1968), a homogeneous sphere in a uniform harmonic magnetic field (Ward, 1969; Ness, 1968) and a two-layered sphere confined by a medium allowing a surface current density and excited by a uniform time-varying magnetic field (Blank and Sill, 1969).

The model we have used is that of a multi-layered sphere excited by a plane electromagnetic field. The layers are concentric and each layer is assumed to have constant electrical parameters chosen according to best estimates (Ward, 1969). Our choice of this model is dictated less by a certainty of its applicability to the real situation than by an acknowledgment

of its possibility. That is, we wish to inquire how layering would affect our concept of the electromagnetic behavior of the lunar sphere and to what extent the possibility of layering should be considered in the design of an experiment to determine the electrical properties of the lunar interior.

The problem of an homogeneous sphere in a plane electromagnetic field is classical and is well reviewed, with references to the original work, in such textbooks as Stratton (1941), Harrington (1961) and Von Bladel (1964). Wait (1951) and Ward (1953, 1959, 1967) have specialized the solution to a uniform time-varying magnetic field. Wait (1961) has presented the theoretical solution for the layered sphere. Our solution generally follows that of Wait (1961) with only slight differences in formulation and the addition of frequency response curves for layered lunar models.

Theoretical Formulation

The geometry is illustrated in Figure 1. The primary plane wave, which is x-polarized and z-traveling, is incident upon a multi-layered sphere of outer radius 1738 km. The layers are numbered from the outside in, beginning with 0 for the external medium and m for the inner core.

With $e^{-i\omega t}$ time dependence suppressed, we seek to solve, in each medium, the following Maxwell equations:

$$\nabla \times \bar{E}(\bar{x},\omega) = \hat{z}\, \bar{H}(\bar{x},\omega) \tag{1}$$

$$\nabla \times \bar{H}(\bar{x},\omega) = \hat{y}\, \bar{E}(x,\omega) \tag{2}$$

with

$$\hat{z} = i\omega\mu \tag{3}$$

$$\hat{\gamma} = \sigma - i\omega\epsilon \tag{4}$$

Fields which satisfy (1) and (2) may be derived from the two scalar potentials ψ and Φ, which are Transverse Electric (TE) and Transverse Magnetic (TM) respectively, under the condition that ψ and Φ satisfy the scalar Helmholtz equations,

$$(\nabla^2 + k^2)\psi = 0 \tag{5}$$

$$(\nabla^2 + k^2)\Phi = 0 \tag{6}$$

$$k^2 = \hat{\gamma}\hat{z} = \omega^2\mu\epsilon + i\mu\sigma\omega \tag{7}$$

In terms of the potentials, the fields are given by

$$\bar{E}(\bar{x},\omega) = \nabla\times\psi r\bar{e}_r + \frac{1}{\hat{\gamma}}\nabla\times\nabla\times\Phi r\bar{e}_r \tag{8}$$

$$\bar{H}(\bar{x},\omega) = \nabla\times\Phi r\bar{e}_r + \frac{1}{\hat{z}}\nabla\times\nabla\times\psi r\bar{e}_r \tag{9}$$

where $\bar{e}_r$ is the unit vector in the r direction of the spherical coordinate system with origin at the center of the sphere.

Following Van Bladel (1964), we may expand the primary plane

wave, assumed to be of unit amplitude, in terms of its potentials as

$$\Phi_p = j\left(\frac{y_0}{z_0}\right)^{1/2} \sum_{n=1}^{\infty} (-j)^n \frac{(2n+1)}{n(n+1)} j_n(k_0 r) \cos\varphi \, P_n^1(\cos\theta) \tag{10}$$

$$\psi_p = \sum_{n=1}^{\infty} (-j)^n \frac{(2n+1)}{n(n+1)} j_n(k_0 r) \sin\varphi \, P_n^1(\cos\theta) \tag{11}$$

where j_n is the spherical Bessel function of order n . The solutions for the total potentials in the various layers may be written down using (10) and (11) and the general solution to the Helmholtz equation. For the ith layer, the solution is

$$\Phi^i = j\left(\frac{y_i}{z_i}\right)^{1/2} \cos\varphi \sum_{n=1}^{\infty} (-j)^n \frac{(2n+1)}{n(n+1)} P_n^1(\cos\theta)\left[a_n^i j_n(k_i r) + b_n^i h_n^{(1)}(k_i r)\right] \tag{12}$$

$$\psi^i = \sin\varphi \sum_{n=1}^{\infty} (-j)^n \frac{(2n+1)}{n(n+1)} P_n^1(\cos\theta)\left[c_n^i j_n(k_i r) + d_n^i h_n^{(1)}(k_i r)\right] \tag{13}$$

where $h_n^{(1)}$ is the spherical Hankel function of the first kind. In the outside medium (layer 0) the only incoming wave is the primary field so that $a_n^0 = c_n^0 = 1$. In the inner core (layer m), finiteness at the origin requires that $b_n^m = d_n^m = 0$. The remaining 4m constants (functions of n) may be obtained by the application of the following boundary conditions, which are sufficient to ensure continuity of tangential $\bar{E}$ and $\bar{H}$.

$$\psi^i = \psi^{i-1}\Big|_{r=R_i} \tag{14}$$

$$\Phi^i = \Phi^{i-1}\Big|_{r=R_i} \tag{15}$$

$$\frac{1}{\hat{z}_i}\frac{\partial}{\partial r}\left(r\psi^i\right) = \frac{1}{\hat{z}_{i-1}}\frac{\partial}{\partial r}\left(r\psi^{i-1}\right)\Bigg|_{r=R_i} \tag{16}$$

$$\frac{1}{\hat{y}_i}\frac{\partial}{\partial r}\left(r\Phi^i\right) = \frac{1}{\hat{y}_{i-1}}\frac{\partial}{\partial r}\left(r\Phi^{i-1}\right)\Bigg|_{r=R_i} \tag{17}$$

Since we are interested in solutions outside the sphere, the problem may be stated to be the determination of the coefficients b_n^0 and d_n^0 as continuous functions of frequency and discrete functions of n. It is convenient to determine these coefficients separately and in a recursive manner, as follows for the potential ψ .

At the inner boundary, $r = R_m$, between the core and the $(m-1)$th layer, equations (14) and (16) comprise two equations in three unknowns which may be combined to yield

$$d_n^{m-1} = r_{n\psi}^m c_n^{m-1} \tag{18}$$

where we designate $r_{n\psi}^m$ as the reflection coefficient from the mth layer for the nth mode of the TE potential ψ . Explicitly, $r_{n\psi}^m$, for an m layer sphere is found to be

$$r_{n\psi}^m = \frac{\hat{z}_m \alpha_n(y_m) j_n(x_m) - \hat{z}_{m-1} j_n(y_m) \alpha_n(x_m)}{\hat{z}_{m-1} h_n^{(1)}(y_m) \alpha_n(x_m) - \hat{z}_m \beta_n(y_m) j_n(x_m)} \tag{19}$$

where

$$\alpha_n(y_m) = \left\{\frac{d}{dy}\left[y\, j_n(y)\right]\right\}_{y=y_m}$$

$$\beta_n(y_m) = \left\{\frac{d}{dy}\left[y\, h_n^{(1)}(y)\right]\right\}_{y=y_m}$$

$$x_m = k_m R_m$$

$$y_m = k_{m-1} R_m$$

and k_i is the propagation constant for the i^{th} medium. At the next boundary out, $r = R_{m-1}$, equations (14), (16) and (18) comprise three equations in four unknowns allowing the relation

$$d_n^{m-2} = r_{n\psi}^{m-1} c_n^{m-2} \tag{20}$$

where $r_{n\psi}^{m-1}$ is found to be

$$r_{n\psi}^{m-1} = \frac{\hat{z}_{m-1} \alpha_n(y_{m-1}) \left[j_n(x_{m-1}) + r_{n\psi}^m h_n^{(1)}(x_{m-1}) \right] - \hat{z}_{m-2} j_n(y_{m-1}) \left[\alpha_n(x_{m-1}) + r_{n\psi}^m \beta_n(x_{m-1}) \right]}{\hat{z}_{m-2} h_n^{(1)}(y_{m-1}) \left[\alpha_n(x_{m-1}) + r_{n\psi}^m \beta_n(x_{m-1}) \right] - \hat{z}_{m-1} \beta_n(y_{m-1}) \left[j_n(x_{m-1}) + r_{n\psi}^m h_n^{(1)}(x_{m-1}) \right]} \tag{21}$$

The recursive relation is now clear; within the i^{th} layer, we may determine $r_{n\psi}^{i+1}$ and hence the relation between d_n^i and c_n^i, if we know $r_{n\psi}^{i+2}$. Beginning at the core, then, we compute $r_{n\psi}^m$ according to equation (19) and proceed outward according to equation (21) until we obtain $r_{n\psi}'$. Since, by the problem formulation, c_n^0 is unity, we have

$$d_n^0 = r_{n\psi}' \tag{22}$$

Equation (19) is a specialization of equation (21), with $r_{n\Psi}^{m+1}$ set to zero (since there is not an $(m+1)^{th}$ layer to give reflection).

The same calculations may be carried out for the TM potential and the results are similar with the only difference being the replacement of $\hat{z}_i$ by $\hat{y}_i$. Thus, the relation for Φ which corresponds to equation (21) is

$$r_{n\Phi}^{m-1} = \frac{\begin{array}{l}\hat{y}_{m-1}\,\alpha_n(y_{m-1})\left[j_n(x_{m-1}) + r_{n\Phi}^{m} h_n^{(1)}(x_{m-1})\right] \\ -\,\hat{y}_{m-2}\, j_n(y_{m-1})\left[\alpha_n(x_{m-1}) + r_{n\Phi}^{m}\beta_n(x_{m-1})\right]\end{array}}{\begin{array}{l}\hat{y}_{m-2}\, h_n^{(1)}(y_{m-1})\left[\alpha_n(x_{m-1}) + r_{n\Phi}^{m}\beta_n(x_{m-1})\right] \\ -\,\hat{y}_{m-1}\,\beta_n(y_{m-1})\left[j_n(x_{m-1}) + r_{n\Phi}^{m} h_n^{(1)}(x_{m-1})\right]\end{array}} \qquad (23)$$

In an identical manner, we may compute $r_{n\Phi}^{1}$ and use the relation

$$b_n^0 = r_{n\Phi}^{1} \qquad (24)$$

With b_n^0 and d_n^0 thus determined, the potentials and hence the fields are theoretically determined everywhere in the space external to the sphere. The method of computation is very similar to that presented by Wait (1961).

It is convenient to regard the TE potential Ψ as an expansion of magnetic multipoles and the TM potential Φ as an expansion of electric multipoles (Jackson, 1962). Neglect of either of the potentials is then equivalent to neglect of either electric or magnetic secondary sources. The conditions under which such an approximation is valid are discussed in the Appendix. For our purpose of illustrating the effect of concentric

layering, we will utilize only the TE potential ψ , thus retaining only the magnetic secondary sources. This choice allows an exact solution if the radial component of $\bar{H}$ is the measured component and has the added advantage of easy comparison with previously computed results (e.g. Wait, 1951; Ward, 1953; Blank and Sill, 1969; Ward, 1967; Wait, 1969).

Calculated Results

For purposes of computation, it is convenient to define a new TE "reflection coefficient" as the ratio of the secondary potential to the primary potential evaluated at the surface of the sphere, for each magnetic multipole. In terms of the calculated coefficient d_n^0 for the solution in the external medium, this reflection coefficient is

$$R_{n\psi} = d_n^0 \frac{h_n^{(1)}(k_0 R_1)}{j_n(k_0 R_1)} \tag{25}$$

where k_0 is the propagation constant of the external medium and R_1 is the outer radius of the first layer.

In order to illustrate the effect of layering, we will make a comparison with the solution for the homogeneous sphere. Figures 2 and 3 portray the frequency behavior of the TE reflection coefficient for two homogeneous spheres of conductivities 1 mho/m and 10^{-4} mhos/m, respectively. The spheres are of lunar size, with radius of 1738 km and have permittivity equal to that of free space. The spheres are non-magnetic and we have chosen free space for the external medium. This choice is not intended to represent an approximation to the behavior of the interplanetary medium, but is merely a convenience to compare homogeneous and layered responses.

For all models, we have calculated the reflection coefficient for each of the first four terms in the series solution and have designated these by modes 1 through 4 in the figures.

The n = 1 curves of Figures 2 and 3 are exactly comparable to those obtained by Wait (1951) and Ward (1953, 1959) and, for later comparison with layered models, we may note certain features of these curves. The first mode, or dipole term, behaves as would be predicted by utilizing a uniform time-varying magnetic field as a source. The peak in the quadrature component of the first (dipole) mode appears at the frequency for which $|K|R \cong \pi$, where K is the propagation constant for the sphere. One may show that this frequency is also that which corresponds to the "Cowling time" (Ness, 1967) for a sphere. The quadrature components of the higher modes exhibit peaks at successively higher frequencies with successively lower amplitudes. The real part, or in-phase component for each mode saturates to -1. In this frequency range, the sphere behaves as a perfect conductor; i.e. total TE potential and radial component of $\bar{H}$ reduce to zero at the surface of the sphere.

In the series solution, equation (13), higher order modes are reduced by the factor $j_n(\kappa_0 R)(2n+1)/n(n+1)$ at the surface of the sphere. This tends to make the first term dominant at the surface for $\kappa_0 R \ll 1$. The Appendix considers the question of neglect of higher order multipoles in some detail.

Figure 3 shows the same characteristics as Figure 2 except for a shift of the diagnostic part of the curves to higher frequencies, which reflects the lower conductivity. Wait (1951) and Ward (1953) have plotted the dipole response versus induction number, $|K|R$, and it is evident

from their curves that, as conductivity decreases, the frequency at which $|K_1 k| = \pi$ increases. Figures 2 and 3 reflect this behavior.

Figures 4 through 6 illustrate the calculated frequency response for three layered models. The particular models are based upon estimates by Ward (1969) and Ward and Jiracek (1969). Their estimates, in turn, have been based upon laboratory measurements of the electrical properties of terrestrial rocks. Because such measurements have often exhibited marked frequency dependence and the frequency range we are considering has not been thoroughly investigated, our models involve substantial extrapolation and are intended to represent only gross estimates based upon meager information.

The calculated reflection coefficient involves computation of equation (21) iteratively through the several layers. The complicated nature of equation (21) and the finite accuracy of the computer combine to yield certain difficulties in the numerical computation. These difficulties appear most often in the form of indeterminate quantities; the numerator and denominator of equation (21) appear so small as to become effectively zero, although the quotient remains finite. The range of uncertain results is noted on each figure and does not affect the major results.

Figure 4 illustrates the reflection coefficient evaluated at the lunar surface for our Model 1. The model consists of 10 m of debris, 90 m of dry rock, 2.9 km of a permafrost layer, 97 km of inner "wet" shell, and a hot conductive core, all with electrical parameters as noted on the figure.

The most distinctive feature of Figure 4 is the appearance of two responses which are well separated in frequency. The first response occurs at $f = 5 \times 10^{-6}$ Hz, where the quadrature peak is used for location.

Making use of the criterion that $|K|R \doteq \pi$ at the peak, and letting $|K| \doteq \sqrt{4\pi\omega}$, we find that $\sigma \doteq 10^{-1}$ mhos/m and thus interpret this response as due to the core alone, the outer layers appearing transparent at the lowest frequencies. The form of the response is very similar to that of a homogeneous sphere of conductivity 10^{-1} mhos/m with the following differences. The peak values of the quadrature and in-phase responses are less than those of Figures 2 and 3, and the "fall-off" of peak values, with increasing mode, is faster. This is a result of being some distance away, through the outer layers, from the anomaly-producing body and indicative of the increasing "fall-off" of higher order multipoles. The further away the observer is from the anomaly-producing body, the more dominant the dipole term becomes, within the quasi-static range. The relative contributions of the several modes is, in fact, a measure of the distance from the surface of the core to the surface upon which the field (or potential) is observed.

Centered at about 1 Hz, we have indicated a range of difficulties in computation where, in the iterative calculation through the layers, the quotient of equation (21) appears indeterminant. At about 10 Hz, the response from the entire lunar sphere appears. Since the potential is evaluated at the surface of the sphere, the in-phase components now saturate to -1, as with the homogeneous models. At the high frequency, we have plotted only modes 1 and 4 for clarity. Mode 4 exhibits the largest response since it was most attenuated in the core response and must recover to the saturation value of -1. Interpretation of this latter response on the basis of a homogeneous model, utilizing the criterion $|K|R \doteq \pi$ at the quadrature peak, would yield a conductivity for the entire sphere of about

10^{-7} mhos/m.

Model 2, the reflection coefficient of which is illustrated in Figure 5, is a particularly high conductivity model. The model consists of an outer layer of debris, three layers of wet rock with the same conductivity but increasing dielectric constant, and a hot conductive core of conductivity 10 mhos/m. The core response occurs at about 10^{-7} Hz and this is unfortunately in the range of computational difficulties. However, the values on either side of the questionable range and the arguments presented for the previous model substantiate that a response does occur in this range. Interpretation of the second response as that of a homogeneous sphere would yield a conductivity estimate of about 10^{-4} mhos/m and this, when compared to the core conductivity, an error of about five orders of magnitude.

Figure 6 illustrates the frequency behavior for Model 3, which is a "warm" moon of low conductivity. Only modes 1 and 4 are presented for clarity. The model consists of a very resistive outer shell of debris, a layer of resistive dry rock, a "moist" (approximately 1% water) shell, and a core with conductivity of 10^{-5} mhos/m. The core response, because of the low assumed conductivity, appears at about 10^{-2} Hz and is followed by a superposition of small amplitude oscillations which we presume to be due to the spherical dielectric waveguide formed by the layer surrounding the core. The entire lunar sphere responds at about 10^{2} Hz with an apparent conductivity of about 10^{-8} mhos/m.

Discussion and Conclusions

We have presented the low frequency behavior for three layered

models, all of which are debatable as regards their accuracy with respect to the moon. However, our information is sufficiently meager that any proposed model would be debatable. We present these layered models only as possibilities in order to show what effect layering might have on a simple interpretation based upon an assumption of homogeneity. Our models have consisted of relatively thin layers near the surface and exhibit two responses; one due to the conductive core and another due to the combination of outer layers and core. Recognition of only the latter feature and interpretation of this feature as induction in the core may lead to a large error in estimating the conductivity of the core. It is clear that the possibility, at least, of layering in the moon should be recognized for the purpose of investigating the lunar response to the low frequency, time-varying interplanetary magnetic field.

APPENDIX

Field Expressions and Quasi-Static Approximations

For convenience, we may rewrite the solutions for the potentials in the external medium as

$$\Phi^0 = j\left(\frac{\hat{y}_0}{j\hat{z}_0}\right)^{1/2} \sum_{n=1}^{\infty} c_n f_n(\theta,\varphi)\left[j_n(k_0 r) + b_n h_n^{(1)}(k_0 r)\right] \tag{A.1}$$

$$\psi^0 = \sum_{n=1}^{\infty} c_n g_n(\theta,\varphi)\left[j_n(k_0 r) + d_n h_n^{(1)}(k_0 r)\right] \tag{A.2}$$

where (r, θ, φ) = coordinates of observer relative to center of sphere

$k_0, \hat{y}_0, \hat{z}_0$ = properties of the external medium as defined in the text. For the purpose of this discussion, these are not necessarily free space values.

$$c_n = (-j)^n (2n+1)/n(n+1) \tag{A.3}$$

$$g_n(\theta,\varphi) = \sin\varphi\, P_n^1(\cos\theta) \tag{A.4}$$

$$f_n(\theta,\varphi) = \cos\varphi\, P_n^1(\cos\theta) \tag{A.5}$$

In terms of the reflection coefficients evaluated at the surface of the sphere, the coefficients are

$$b_n = R_{\Phi n}\,\frac{j_n(k_0 R)}{h_n^{(1)}(k_0 R)} \tag{A.6}$$

$$d_n = R_{\psi n} \frac{j_n(k_0 R)}{h_n^{(1)}(k_0 R)} \tag{A.7}$$

where R is the outer radius of the sphere.

Equations (8) and (9) in the text provide the relationship between the fields and potentials. Our interest will be confined to only the magnetic fields and we will designate the field components as follows:

H_u^{Φ} = contribution of the potential Φ to the u component of magnetic field.

H_u^{ψ} = contribution of the potential ψ to the u component of magnetic field.

$H_u = H_u^{\Phi} + H_u^{\psi}$ = u component of magnetic field.

The expansion of equation (9) yields, for the three magnetic field components in the external medium,

$$H_r = \frac{1}{\hat{z}_0} \frac{1}{r \sin\theta} \left[-\frac{\partial}{\partial\theta}\left(\sin\theta \frac{\partial \psi^e}{\partial\theta}\right) - \frac{1}{\sin\theta} \frac{\partial^2 \psi^e}{\partial \varphi^2} \right] \tag{A.8}$$

$$H_\theta = \frac{1}{\sin\theta} \frac{\partial \Phi^e}{\partial \varphi} + \frac{1}{\hat{z}_0} \frac{1}{r} \frac{\partial}{\partial r}\left(r \frac{\partial \psi^e}{\partial \theta}\right) \tag{A.9}$$

$$H_\varphi = -\frac{\partial \Phi^e}{\partial \theta} + \frac{1}{\hat{z}_0} \frac{1}{r} \frac{\partial}{\partial r}\left(\frac{r}{\sin\theta} \frac{\partial \psi^e}{\partial \varphi}\right) \tag{A.10}$$

In equations (A.9) and (A.10), the two terms are, respectively, H_u^{Φ} and H_u^{Ψ} . The r component, equation (A.8), contains only H_r^{Ψ} , which is a reflection of the transverse magnetic nature of $\underline{\Phi}$.

Performing the differentiation, the field components are, explicitly,

$$H_r^{\Psi} = \frac{1}{\hat{z}_0 r} \sum_{n=1}^{\infty} (2n+1) \left[j_n(k_0 r) + d_n h_n^{(1)}(k_0 r) \right] \sin\varphi \, P_n^1(\cos\theta) \tag{A.11}$$

$$H_r^{\Phi} = 0 \tag{A.12}$$

$$H_\theta^{\Psi} = \sum_{n=1}^{\infty} c_n \frac{\sin\varphi}{\sin\theta} \left[n \cos\theta \, P_n^1(\cos\theta) - (n+1) P_{n-1}^1(\cos\theta) \right] \cdot$$

$$\cdot \left\{ \frac{-n}{\hat{z}_0 r} \left[j_n(k_0 r) + d_n h_n^{(1)}(k_0 r) \right] + \frac{k_0}{\hat{z}_e} \left[j_{n-1}(k_0 r) + d_n h_{n-1}^{(1)}(k_0 r) \right] \right\} \tag{A.13}$$

$$H_\theta^{\Phi} = -j \frac{\sin\varphi}{\sin\theta} \left(\frac{\hat{y}_0}{\hat{z}_0} \right)^{1/2} \sum_{n=1}^{\infty} c_n P_n^1(\cos\theta) \left[j_n(k_0 r) + b_n h_n^{(1)}(k_0 r) \right] \tag{A.14}$$

$$H_\varphi^{\Psi} = -\sum_{n=1}^{\infty} c_n \frac{\cos\varphi}{\sin\theta} P_n^1(\cos\theta) \left\{ \frac{-n}{\hat{z}_0 r} \left[j_n(k_0 r) + d_n h_n^{(1)}(k_0 r) \right] + \frac{k_0}{\hat{z}_0} \left[j_{n-1}(k_0 r) + d_n h_{n-1}^{(1)}(k_0 r) \right] \right\} \tag{A.15}$$

$$H_\varphi^{\bar{E}} = -j\left(\frac{y_0}{z_0}\right)^{1/2} \sum_{n=1}^{\infty} c_n \frac{\cos\varphi}{\sin\theta}\left[j_n(k_0 r) + b_n h_n^{(1)}(k_0 r)\right]\left[n\cos\theta\, P_n'(\cos\theta) - (n+1) P_{n-1}'(\cos\theta)\right] \tag{A.16}$$

By equations (A.11) through (A.16), the fields are described everywhere, though not in a very convenient form. Our interest, however, is basically with the secondary field as expressive of the electrical nature of the entire sphere. This confines us, by skin depth arguments, to wavelengths which are much larger than the dimension of the sphere. This may be stated as $|k_0| R \ll 1$. Further, we are interested in observations which are within a distance of the sphere which is very much less than a wavelength. This condition may be stated as $|k_0| r \ll 1$. These conditions lead to substantial simplification.

Consider first the relative contributions in equations (A.13) and (A.15), of the secondary field terms in $h_n^{(1)}(k_0 r)$ and $h_{n-1}^{(1)}(k_0 r)$. The ratio of the term in $h_{n-1}^{(1)}(k_0 r)$ to that in $h_n^{(1)}(k_0 r)$ is given by

$$\alpha = \frac{k_0 r}{n} \frac{h_{n-1}^{(1)}(k_0 r)}{h_n^{(1)}(k_0 r)} \tag{A.17}$$

Using small argument expansions for the Hankel functions, we obtain

$$\lim_{k_0 r \to 0} \alpha = \frac{(k_0 r)^2}{n(2n-1)} \tag{A.18}$$

For $(k_0 r)$ small, the term $h_n^{(1)}(k_0 r)$ is dominant for each n and becomes more dominant as n increases. The term in $h_{n-1}^{(1)}(k_0 r)$ is then negligible

for $(\kappa_c r)$ small. Physically, this is equivalent to the quasi-static approximation in the near field of a multipole.

We now consider the relative contributions of Ψ and Φ to the tangential magnetic field. Neglecting the ϕ dependence, the ratio of secondary field components is

$$\frac{H_{\theta sc}^{\Phi}}{H_{\theta sc}^{\Psi}} = \frac{H_{\varphi sc}^{\Phi}}{H_{\varphi sc}^{\Psi}} = \frac{\left(\frac{\hat{\mu}_c}{\hat{\epsilon}_c}\right)^{1/2} b_n h_n^{(1)}(\kappa_c r)}{\frac{n}{\hat{\epsilon}_c r} d_n h_n^{(1)}(\kappa_c r)} = \frac{b_n}{d_n} \frac{\kappa_c r}{n} = \frac{K_{\Phi n}}{K_{\Psi n}} \frac{\kappa_c r}{n} \qquad \text{(A.19)}$$

$K_{\Phi n}$ has not been plotted for this report but, in the frequency range of interest, is a constant of order 1. Thus, in the region where $K_{\Psi n}$ is non-zero--i.e. where an induction response occurs--and for $(\kappa_c r)$ small, H_{θ}^{Φ} and H_{φ}^{Φ} are negligible with respect to H_{θ}^{Ψ} and H_{φ}^{Ψ}. The earlier neglect of ϕ dependence does not negate this result since, if ϕ is such that $H_{\theta}^{\Phi} > H_{\theta}^{\Psi}$, then, from equations (A.13) through (A.16), $H_{\varphi}^{\Psi} > H_{\varphi}^{\Phi}$ and, for small $\kappa_c r$, $H_{\varphi}^{\Psi} \gg H_{\theta}^{\Phi}$, and the dominant contribution to the tangential field is still made by Ψ. Physically, this result is a statement of the fact that, in the near field of a magnetic multipole and an electric multipole, the magnetic multipole is the dominant contributor to the magnetic fields.

Lastly, we consider the relative contributions of higher order multipoles. For the three components, the ratio of the secondary field contribution of the (n + 1)th term to that of the n th term may be shown to be proportional to $K_{\Psi(n+1)}(\kappa_c R)^2 / K_{\Psi n}(\kappa_c r)$, neglecting the ϕ dependence. Since $\kappa_c R \leq \kappa_c r$ for observations outside the sphere, and since $|K_{\Psi(n+1)}| \leq |K_{\Psi n}|$ the ratio is small for $\kappa_c R$ small. Physically, this result illustrates the dominance of the dipole term. θ may be such that the dipole contribution

to a particular component is zero while that of some higher order multipole is non-zero. However, in such an instance, the component will be small in comparison to the maximum contribution of the dipole term.

Under these quasi-static approximations, the field components become

$$H_r \cong j\left(\frac{\hat{y}_0}{\hat{z}_0}\right)^{1/2}\left[1 + R_{\psi_1}\frac{R^3}{r^3}\right]\sin\varphi\sin\theta \qquad \text{(A.20)}$$

$$H_\theta \cong -\frac{j}{2}\left(\frac{\hat{y}_0}{\hat{z}_0}\right)^{1/2}\left[1 + R_{\psi_1}\frac{R^3}{r^3}\right]\sin\varphi\cos\theta \qquad \text{(A.21)}$$

$$H_\varphi \cong \frac{j}{2}\left(\frac{\hat{y}_0}{\hat{z}_0}\right)^{1/2}\left[1 + R_{\psi_1}\frac{R^3}{r^3}\right]\cos\varphi \qquad \text{(A.22)}$$

The expressions are thus greatly simplified. The approximations depend heavily on the properties of the outside medium, explicitly on k_e . If we choose k_e to be the propagation constant of free space, such approximations are justified in the lunar case for frequencies below 1 Hz. However, the choice of free space as representative of the interplanetary environment at such frequencies is very questionable. If the lunar environment is reasonably conductive, the quasi-static approximations do not hold and, for this reason, we have computed the first four modal reflection coefficients.

References

Blank, J. L. and Sill, W. R., 1969, Response of the moon to the time-varying interplanetary field, J. Geophys. Res., Vol. 74, No. 3, p. 736.

Harrington, R. F., 1965, Time harmonic electromagnetic fields, McGraw-Hill, New York.

Jackson, J. D., 1962, Classical electrodynamics, Wiley, New York, p. 543.

Ness, N. F., 1967, Early results from the magnetic field experiment on Explorer 35, J. Geophys. Res., Vol. 72, No. 23.

Schwartz, K., 1967, Theoretical problems associated with the use of magnetometers on the moon, American Nucleonics Corp. Rept ANC TM38-1 under NASA Contract NA22-4026.

Stratton, J. A., 1941, Electromagnetic theory, McGraw-Hill, New York.

Van Bladel, J., 1964, Electromagnetic fields, McGraw-Hill, New York, p. 259-262.

Wait, J. R., 1951, A conducting sphere in a time-varying magnetic field, Geophysics, Vol. XVI, No. 4, p. 666.

Wait, J. R., 1961, Electromagnetic scattering from a radially inhomogeneous sphere, Appl. Sci. Res., Section B, Vol. 10, p. 441.

Ward, S. H., 1953, A method for measuring the electrical conductivity of diamond drill core specimens, Geophysics, Vol. XVIII, No. 2, p. 434.

Ward, S. H., 1959, Unique determination of conductivity, susceptibility, size and depth in multifrequency electromagnetic exploration, Geophysics, Vol. XXIV, No. 3, p. 531.

Ward, S. H., 1967, Electromagnetic theory for geophysical applications, in Mining Geophysics, Vol. II, Soc. Explor. Geophys., Tulsa, Oklahoma.

Ward, S. H., Jiracek, G. R. and Linlor, W. I., 1968, Electromagnetic Reflection from a Plane-Layered Lunar Model, J. Geophys. Res., Vol. 73, No. 4.

Ward, S. H., 1969, Gross estimates of the conductivity, dielectric constant and magnetic permeability distribution in the moon, Radio Sci., Vol. 4, No. 2.

Ward, S. H. and Jiracek, G. R., 1969, Personal Communication.

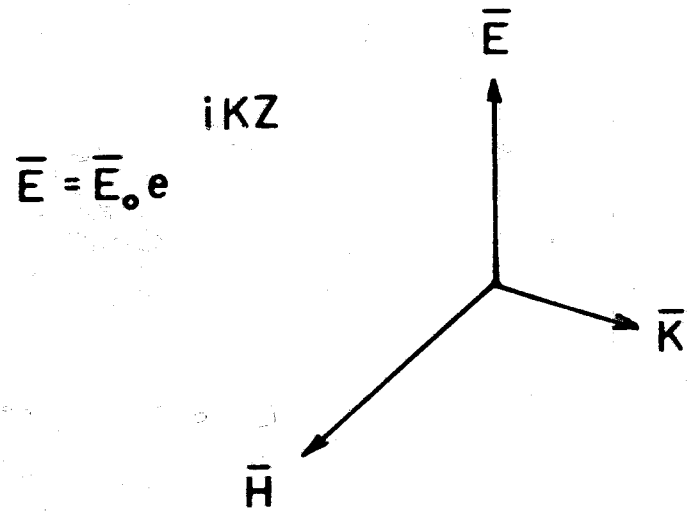

PLANE WAVE INCIDENT FIELD
X-POLARIZED, Z-TRAVELING

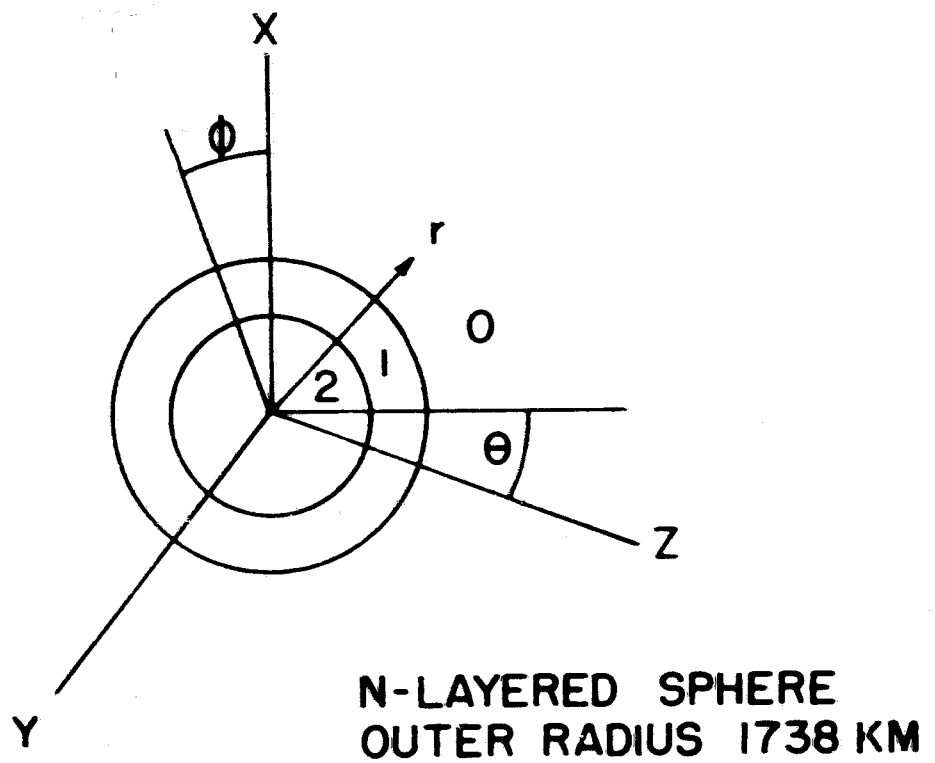

N-LAYERED SPHERE
OUTER RADIUS 1738 KM

FIGURE 1. N-Layered Lunar Model in Plane Wave Electromagnetic Field.

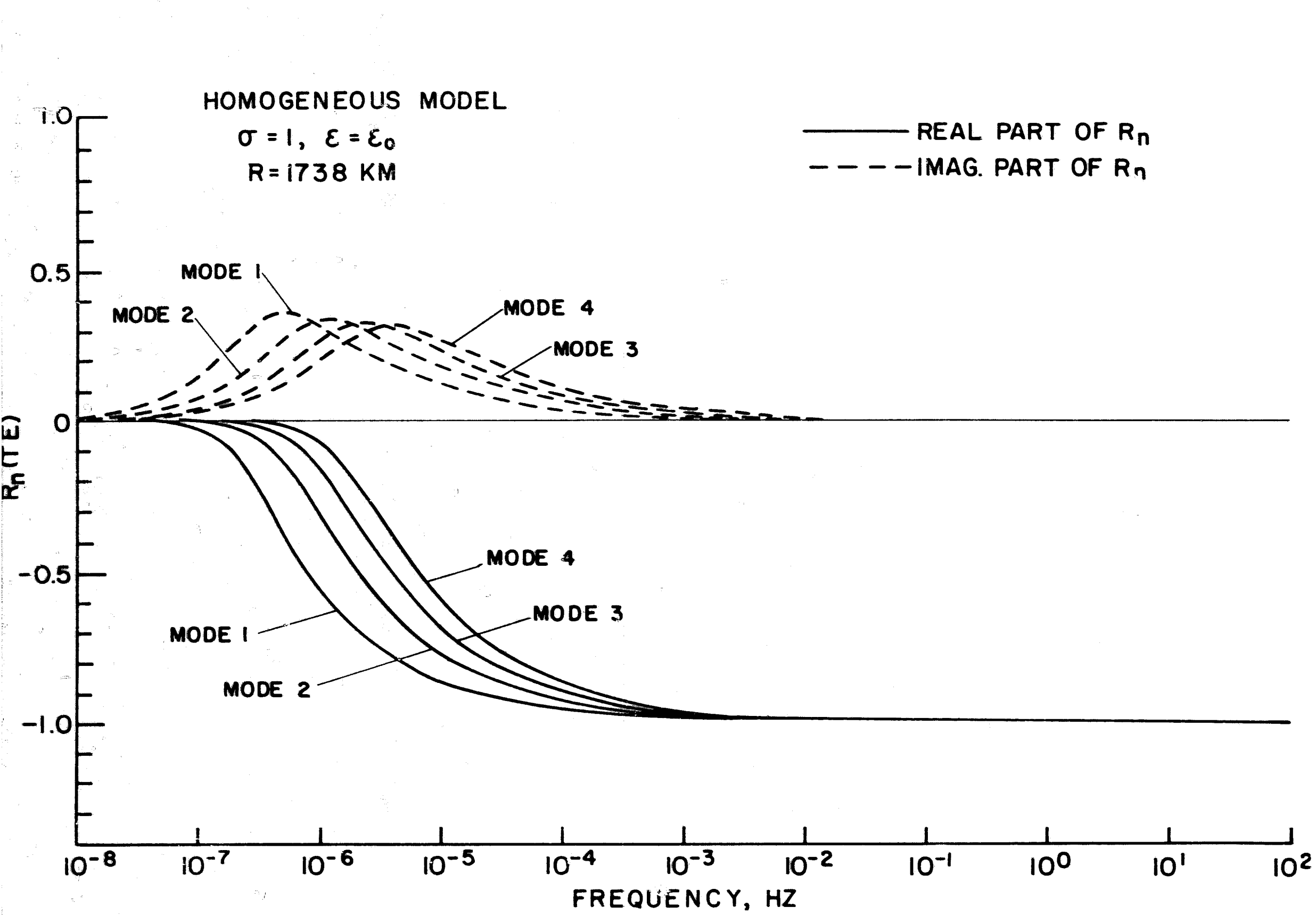

FIGURE 2. Transverse Electric Reflection Coefficients vs. Frequency, for Homogeneous Lunar Model, σ = 1 mho/m.

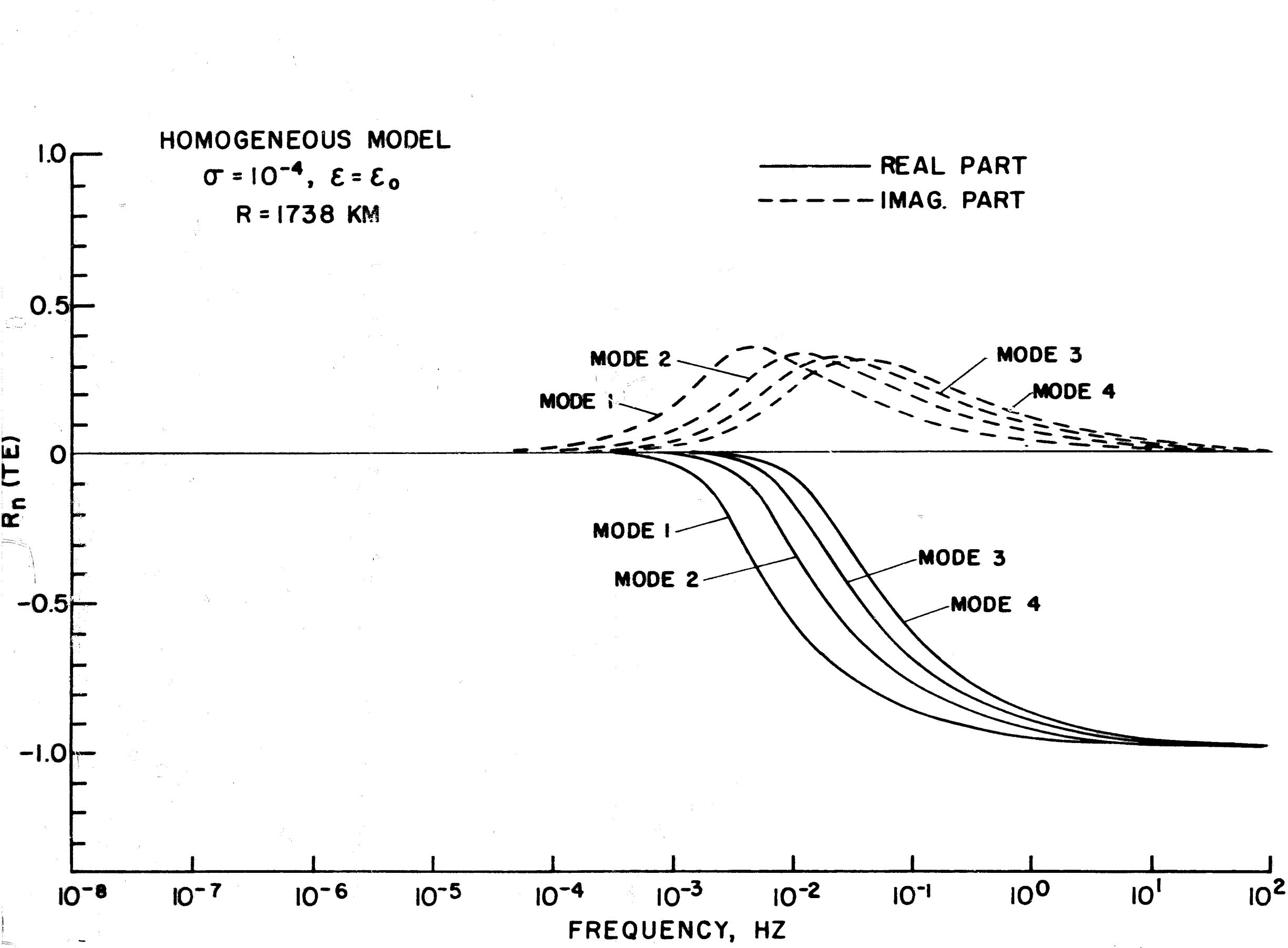

FIGURE 3. Transverse Electric Reflection Coefficients vs. Frequency, for Homogeneous Lunar Model, $\sigma = 10^{-4}$ mho/m.

MODEL 1

0M	FREE SPACE μ_0, ε_0
10M	$\sigma = 5 \times 10^{-11}, \varepsilon = 5\varepsilon_0$
100M	$\sigma = 10^{-10}, \varepsilon = 11\varepsilon_0$
3KM	$\sigma = 5 \times 10^{-5}, \varepsilon = 10^3\varepsilon_0$
10^2 KM	$\sigma = 5 \times 10^{-7}, \varepsilon = 10^3\varepsilon_0$
	$\sigma = 10^{-1}, \varepsilon = 10^4\varepsilon_0$

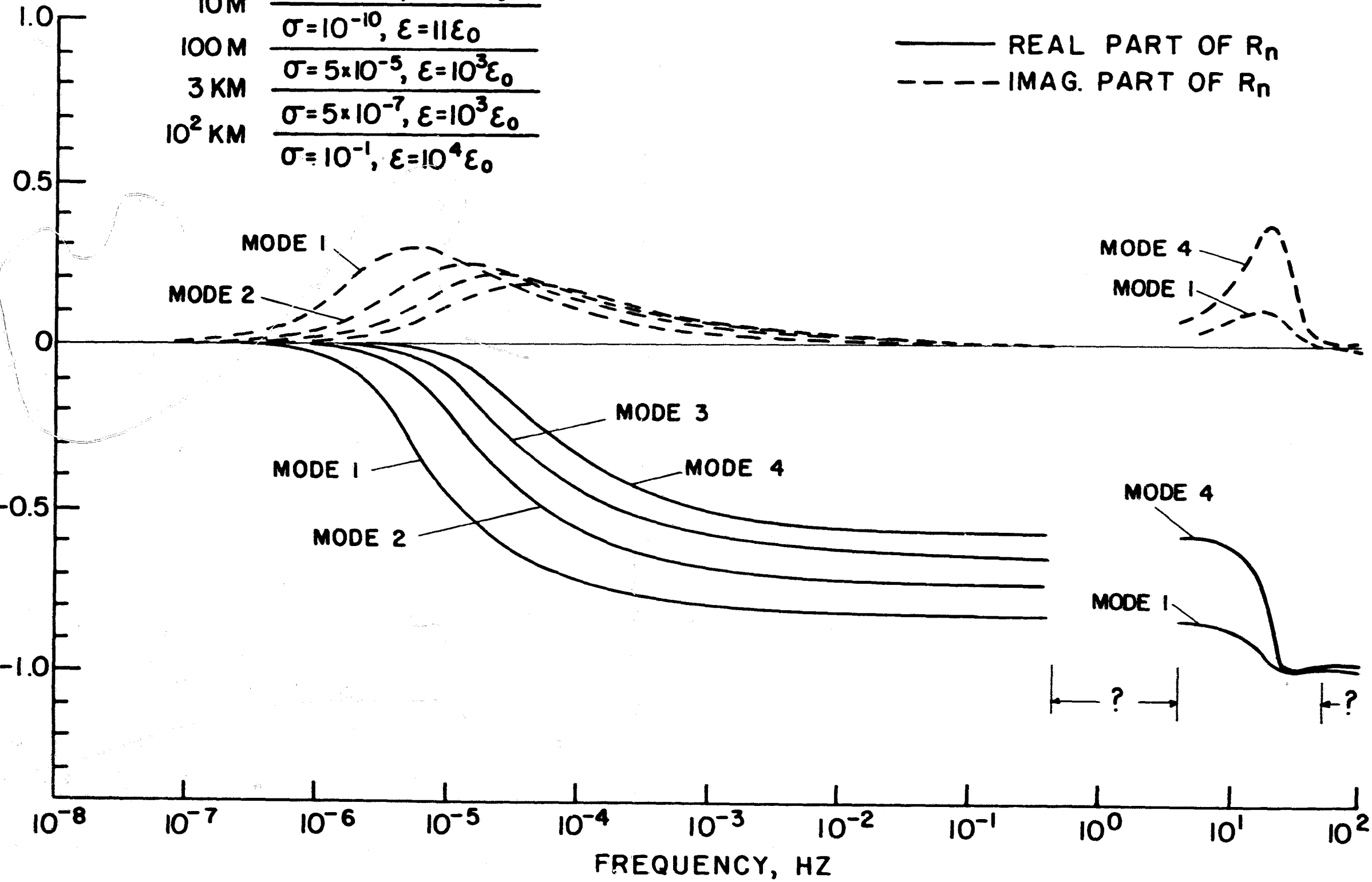

FIGURE 4. Transverse Electric Reflection Coefficients vs. Frequency for Layered Model 1.

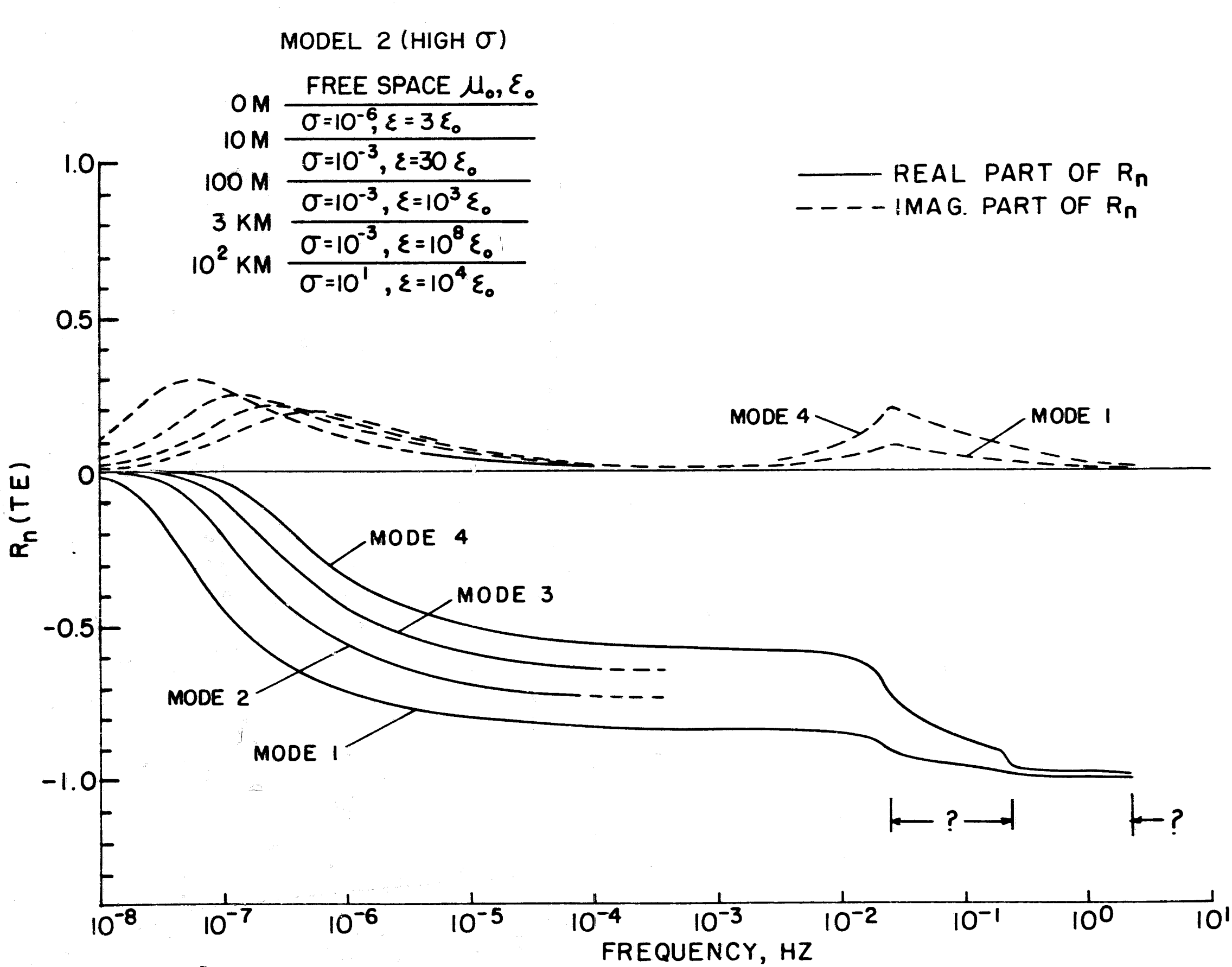

FIGURE 5. Transverse Electric Reflection Coefficients vs. Frequenc, for Layered Model 2.

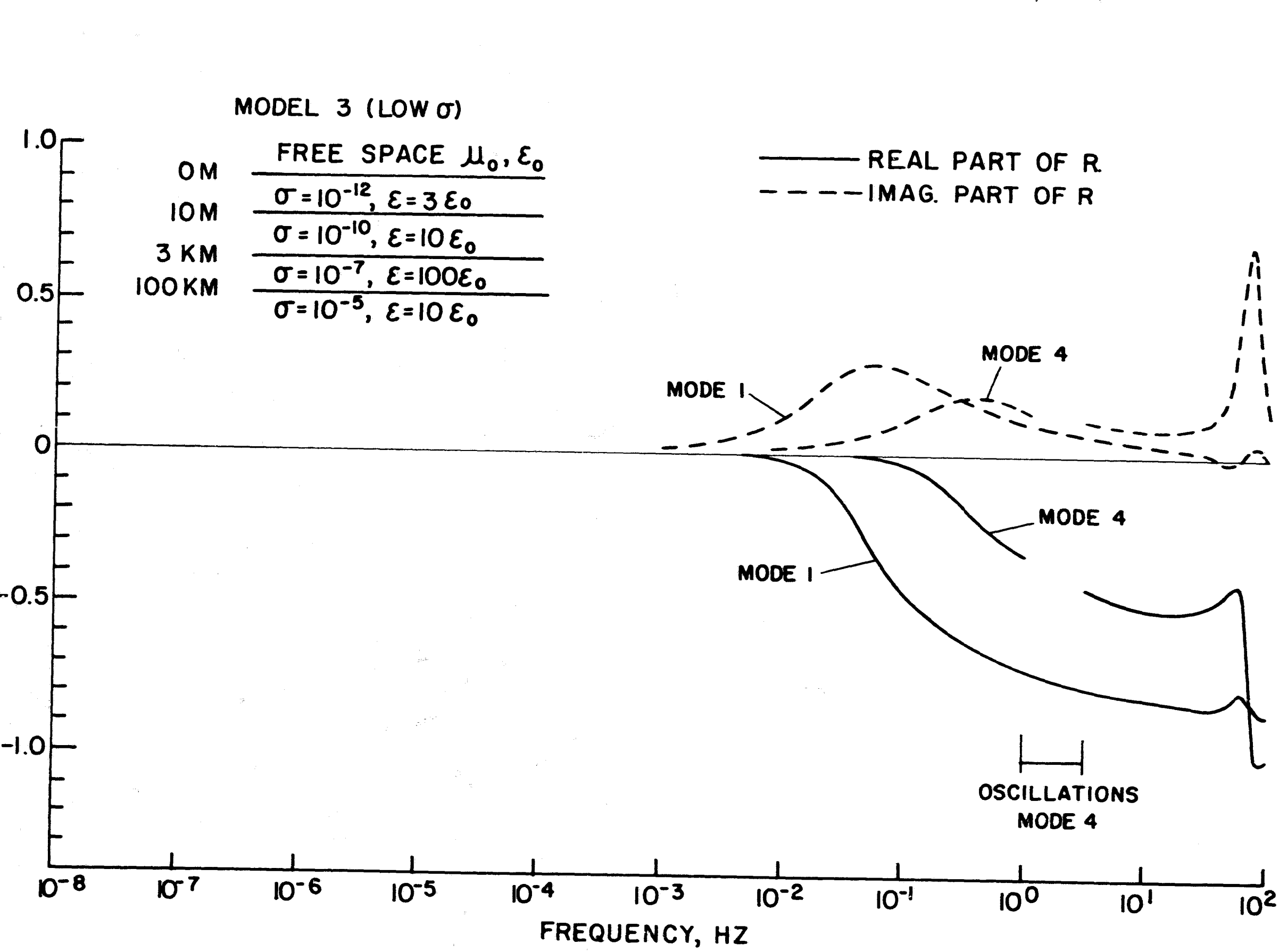

FIGURE 6. Transverse Electric Reflection Coefficients vs. Frequency for Layered Model 3.